# Structural evaluation of FHX for PGSFR at transient condition

Nak-Hyun Kim*, S.K. Kim
*Korea Atomic Energy Research Institute, Daedeok-daero 989-111, Yuseong-gu, Daejeon, 305-335, Korea*
**Corresponding author: nhk@kaeri.re.kr*

## 1. Introduction

A Prototype Gen-IV Sodium-Cooled Fast Reactor (PGSFR) has been under development in Korea since 2012 according to a national nuclear R&D program which aims the construction of a prototype sodium-cooled fast reactor by 2028. The purpose of the PGSFR is to achieve an enhanced safety, an efficient utilization of uranium resources, and a reduction of a radioactive waste volume in Korea [1, 2]. The PGSFR is a pool-type SFR with the capacity of 150 MWe and uses metallic fuel.

Fig. 1 shows the overall configuration of the PGSFR [3]. The DHRSs are composed of two types based on the design concept of diversity and redundancy [4, 5]. For the diversity of the design, one type is an active decay heat removal system (ADHRS) which is operated by active components (e.g. blowers) and the other is a passive decay heat removal system (PDHRS) which operates based on natural convention driving head alone.

Two heat exchangers to be installed in the each ADHRS loop are a forced-draft sodium-to-air heat exchanger (FHX) and a sodium-to-sodium decay heat exchanger (DHX) while two heat exchangers to be installed in the each PDHRS loop are a natural-draft sodium-to-air heat exchanger (AHX) and a DHX. The material of the FHX and AHX is martensitic stainless steel type 9Cr-1Mo-V.

In this paper, a system description for DHRS in PGSFR was provided. And an elevated temperature design and a structural integrity evaluation result of the FHX were described. The finite element analysis was carried out by three-dimensional analysis with ANSYS [6] and structural integrity evaluation was carried out according to the ASME Code B&PV section III Division 5 [7].

## 2. Description of DHRS and FHX

### *2.1 The Decay Heat Removal System*

The DHRS is used to remove the decay heat from the reactor core or from the spent fuel storage after the reactor shutdown when the normal heat transport path is not available. It is a safety-grade system and is designed to have sufficient cooling capability to bring the plant to safe shutdown condition under post-accident conditions. The total heat removal capacity of the DHRS is 10 MWt which amounts to about 2.5% of the rated core thermal power. The DHRS is capable of cooling the plant from an initial temperature corresponding to any power operation condition to the

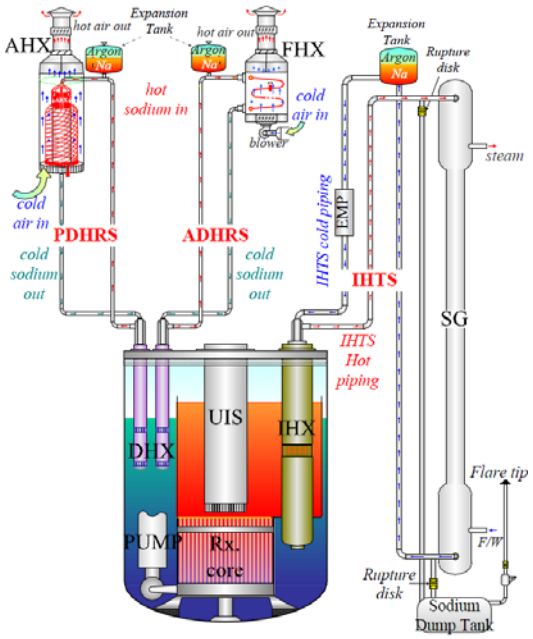


Fig. 1. Schematic diagram and solid modeling for the PGSFR.

safe shutdown condition within 72 hours after reactor shutdown with a single failure. The elevation difference between the DHX and the sodium-to-air heat exchanger (AHX or FHX) in each DHRS sodium loop is sufficiently high to ensure that the natural circulation head in the DHRS sodium loop provides the required sodium flow. Heat is transmitted from the primary cold sodium pool into the DHRS sodium loop via DHX, and a direct heat exchange occurs between the tube-side sodium and the shell-side air through the sodium-to-air heat exchanger tube wall.

### *2.2 The Forced-Draft Sodium-to-Air Heat Exchanger*

The FHX employed in the ADHRS is a shell-and-tube type counter-current flow heat exchanger with serpentine (M-shape) finned-tube arrangement. Liquid sodium flows inside the heat transfer tubes and atmospheric air flows over the finned tubes. The configuration and overall shape of the unit are shown in Figure 2. The material of the FHX is 9Cr-1Mo-V steel. The design pressure and temperature are 0.6 MPa and 470°C, respectively. The outer diameter and thickness of the tube is 34.0 mm and 1.65 mm, respectively. The number of tubes, effective tube length and inclined angle are 96, 8 m and 7.2°, respectively. All of the serpentine (M-shape) tubes have helical fins over the straight tube parts with a density of 152 fins per meter.

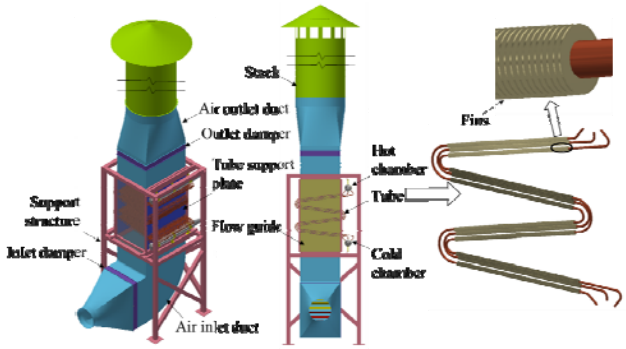


Fig. 2. Configuration of the FHX.

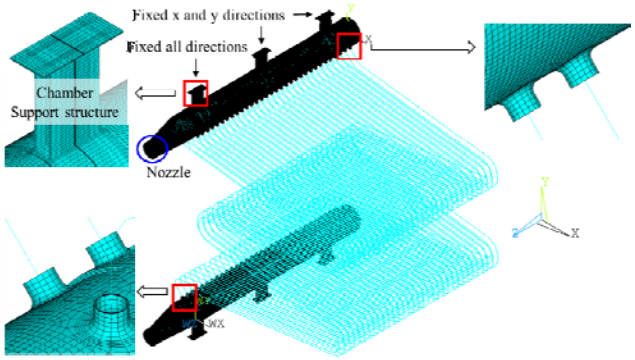


Fig. 3. Finite element model of chamber with tubes in the FHX.

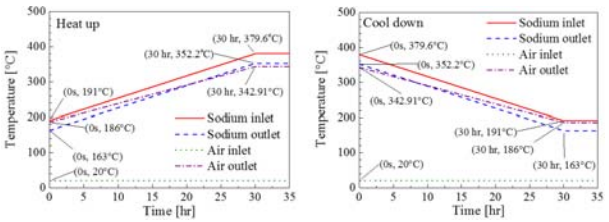


Fig. 4. Transient temperature of the FHX.

## 3. Finite Element Analysis

The FHX consists of support structure, chamber and tubes, etc. The chamber is under a high temperature condition and pressure boundary. Thus, the chamber is the most interested part of structural integrity. In this paper, the structural analysis was performed only for the chamber with tubes.

### *3.1 Finite Element Modeling*

The hot chamber and the cold chamber were fully modeled in the 3D FE model as shown in Fig. 3. For the convenience of analysis, tubes were modeled as pipe elements. Thus, the fin part of the tube was not modeled. However, the fin effect in the finned tube was taken into account by considering equivalent heat transfer area. The outer surface area of the finned tube is eight times higher than that of bare tube. So the finned-tube part was modeled with bare tube with heat transfer coefficient which is eight times larger than that of the bare tube. The total number of nodes was 738,624 and

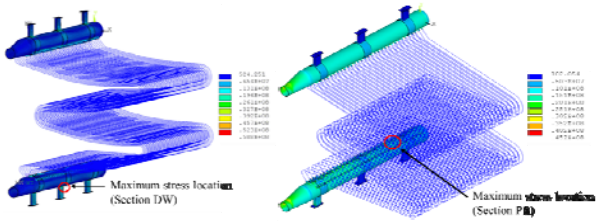


(a) (b)

Fig. 5. Stress analysis results of (a) self-weight and (b) pressure loading.

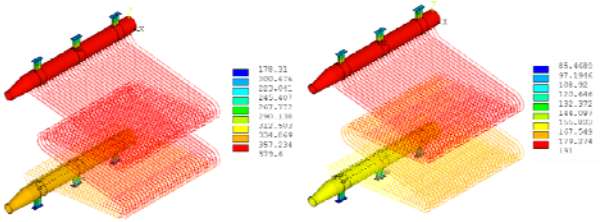

(a) (b)

Fig. 6. Heat transfer analysis results at t=30 hours of (a) heat up and (b) cool down transient.

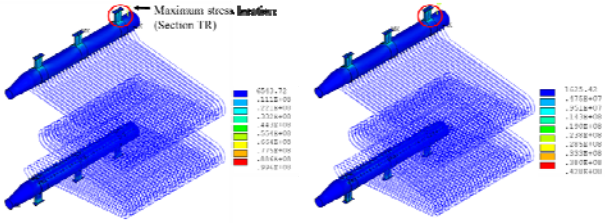


(a) (b)

Fig. 7. Thermal stress analysis results at t=30 hours of (a) heat up and (b) cool down transient.

the total number of elements (3D and pipe element) was 569,956.

As the loading conditions, the transients for the sodium and air was assumed as shown in Fig. 4. The transient time was conservatively assumed to be 30 hours.

As boundary conditions, the bottom surface of the chamber support structure near the nozzle was completely fixed. However, since the other chamber support structures slide axially in order to accommodate axial thermal expansion of the chamber, the other two bottom surfaces were fixed in x and y directions. Using the CERIG option [6], the three-dimensional elements of the chambers were connected to the pipe elements of the tubes. The nodes of the nozzle end were constrained to move only in the radial direction from the nodes of the end of the pipe element.

### *3.2 Finite Element Results*

Primary and secondary stress analyses were performed. A commercial finite element analysis program, ANSYS [6], was used for the analysis. The self-weight and the pressure loading were considered as primary loads, the transient temperature in Fig. 4 was considered as secondary load. The stress analysis

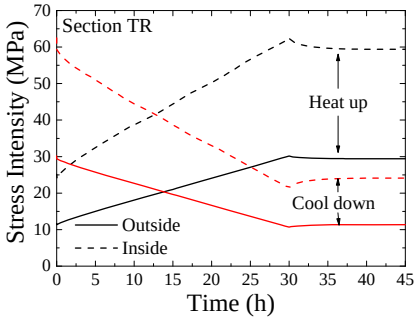


Fig. 8. Stress intensity at maximum stress location during transient

results of self-weight and pressure loading are shown in Fig. 5. As a result of the self-weight loading analysis result, the maximum stress intensity was 58.8 MPa in the middle chamber support structure of the cold chamber as shown in Fig. 5(a). As a result of the pressure loading analysis result, the maximum stress intensity was 45.2 MPa in the nozzle of the cold chamber as shown in Fig. 5(b).

The overall temperature distribution of the chamber at t=30 hours of heat up and cool down transients are shown in Fig. 6, which shows a gradual change in the temperature distribution along the axial direction of the tubes. These temperature distribution were used for thermal stress analysis.

A stress analysis taking the temperature distributions into account was conducted for the chamber with tubes. The stress distributions of the chamber at 30 hours after the start of heat up show that the maximum stress intensity at the chamber support structure in Fig. 7(a) was 62 MPa. At 30 hours after the start of cool down, the maximum stress location is same as the heat up transient and the value is 22 MPa. The change in stress intensity at maximum stress location during transient is shown in Fig. 8.

## 4. Evaluation Results

According to the ASME Code B&PV Section III Division 5 Subsection HB, subsection A provides rules for design at low temperature condition and subsection B provides rules for design at elevated temperature design. Therefore, the structural evaluation was performed separately for low and elevated temperature. For 9Cr-1Mo-V materials, the criterion for low and elevated temperature is 375ºC.

### *4.1 Low Temperature Condition*

In the self-weight and pressure loading analysis, the maximum stress location is the chamber support structure. The maximum temperature where the maximum stress occur is lower than 375ºC in transient condition. Therefore, it was evaluated according to ASME Code B&PV Section III Division 5 Subsection HB Subpart A because it is a low temperature condition. The primary and secondary stresses evaluation results

Table I: Evaluation results of FHX at low temperature condition

| Sections | Node | Evaluation items | Calculated (MPa) | Limit (MPa) | Margin | Max. Temp. (ºC) | Code |
|---|---|---|---|---|---|---|---|
| DW | 549460 | $P_L+P_b+P_e+Q$ | 12.8 | 572.6 | 44 | 351.6 | ASME Sec. III Div.5-HBA |
| | | Thermal Stress Ratchet | 9.7 | 28116.1 | 2904 | | |
| | 542812 | $P_L+P_b+P_e+Q$ | 14.5 | 572.9 | 39 | 350.4 | |
| | | Thermal Stress Ratchet | 23.9 | 28116.1 | 1174 | | |
| PR | 507408 | $P_L+P_b+P_e+Q$ | 20.2 | 572.5 | 27 | 352 | |
| | | Thermal Stress Ratchet | 4.3 | 8196.1 | 1892 | | |
| | 507375 | $P_L+P_b+P_e+Q$ | 12.5 | 572.5 | 45 | 352 | |
| | | Thermal Stress Ratchet | 2.5 | 8196.1 | 3239 | | |

Table II: Evaluation results of FHX at elevated temperature condition

| Sections | Node | Evaluation items | | Calculated | Limit | Margin | Max. Temp. (ºC) | Code |
|---|---|---|---|---|---|---|---|---|
| TR | 355265 | $P_m$ (MPa) | | 4.9 | 182.2 | 36 | 377.8 | ASME Sec. III Div.5-HBB |
| | | $P_L+P_b$ (MPa) | | 6.8 | 273.3 | 39 | | |
| | | $P_L+P_b/k_t$ (MPa) | | 6.4 | 314.6 | 48 | | |
| | | UFS($t_i/t_{im}$) | | 525600 | 26989000 | 50 | | |
| | | UFS($t_i/t_{ib}$) | | 525600 | 26862000 | 50 | | |
| | | Inelastic strain | | 0.082 | 1.0 | 11 | | |
| | | Damage | Fatigue | <0.0001 | intersection (0.1,0.01) | - | | |
| | | | Creep | 0.026 | | | | |
| | 355327 | $P_m$ (MPa) | | 4.9 | 182.1 | 36 | 377.8 | |
| | | $P_L+P_b$ (MPa) | | 3.5 | 273.1 | 76 | | |
| | | $P_L+P_b/k_t$ (MPa) | | 3.6 | 313.2 | 87 | | |
| | | UFS($t_i/t_{im}$) | | 525600 | 23880000 | 44 | | |
| | | UFS($t_i/t_{ib}$) | | 525600 | 23985000 | 45 | | |
| | | Inelastic strain | | 0.105 | 1.0 | 9 | | |
| | | Damage | Fatigue | <0.0001 | intersection (0.1,0.01) | - | | |
| | | | Creep | 0.023 | | | | |

are shown in Table I. The section DW and PR in the table are the section of maximum stress location in the self-weight and pressure loading analysis, respectively, as shown in Fig. 5. The calculated stresses in all sections satisfy the criteria of the ASME code.

### *4.2 Elevated Temperature Condition*

As shown in Fig. 6(a), the temperature of the hot chamber is above 375ºC during the transient. Therefore, it was evaluated according to ASME Code Section III Division 5 Subsection HB Subpart B because it is an elevated temperature condition. The evaluation results are shown in Table II. The section TR in the table is the section of maximum stress location in the thermal stress analysis as shown in Fig. 7. The calculated values satisfy not only stress limits but also strain limit with sufficient margin. Evaluation results of the creep-fatigue damage for the FHX showed that damage under creep and fatigue loading was negligible and the integrity of the FHX was confirmed.

## 5. Conclusions

A high temperature design and structural analyses of the FHX were carried out and its structural integrity was evaluated per ASME Code rule. The FHX employed in the ADHRS is a shell-and-tube type counter-current flow heat exchanger with serpentine (M-shape) finned-tube arrangement.

Three-dimensional finite element analyses were conducted for the FHX, and primary stress, inelastic strain and creep-fatigue damage at several locations were evaluated according to the elevated temperature design codes, ASME Code B&PV Section III Division 5. The present design of the FHX was shown to be acceptable for a transient condition according to the design code. The highest stress intensity under self-weight and pressure loading were calculated to be 58.8 MPa at the chamber support structure and 45.2 MPa at nozzle. The maximum thermal stress during transient is 62 MPa at the hot chamber.

Structural integrity evaluation was carried out for low and high temperature conditions according to the ASME code. In the low temperature condition, only the primary stress was evaluated. In the high temperature condition, not only the primary stress limits but also the inelastic strain and creep-fatigue damage were evaluated. The calculated values satisfy all limits with sufficient margin. Evaluation results of the creep-fatigue damage for the FHX showed that damage under creep and fatigue loading was negligible and the structural integrity of the FHX was confirmed.

## Acknowledgements

This study was supported by the National Research Foundation of Korea grant funded by the Korea government (Ministry of Science, ICT and Future Planning).

## REFERENCES

[1] K.H. KOO, “Status of the fast reactor technology development in Korea”, 48th TWG-FR Meeting, Obninsk, Russia, May 25-29 (2015).
[2] J.W. YOO, et al., “Overall reactor system description of prototype gen-IV sodium cooled fast reactor”, Transactions of 2016 ANS Annual Meeting, New Orleans, USA, June 12-16 (2016).
[3] K.H. KOO, “Mechanical Design of Prototype Gen-IV Sodium Cooled Fast Reactor”, KAERI, KAERI/RR-4048/2015, Daejeon (2015),
[4] Y.I. KIM, et al., “Sodium cooled fast reactor development in Korea”, FR-13, Paris, March 4-7 (2013)
[5] T.H. LEE, et al., “Fluid System Design of Prototype Gen-Ⅳ Sodium Cooled Fast Reactor”, KAERI, KAERI/RR-4044/2015, Daejeon (2015)
[6] ANSYS, ANSYS User’s manual, Release 15.0, ANSYS Inc. (2015).
[7] THE AMERICAN SOCIETY OF MECHANICAL ENGINEERS, ASME Boiler and Pressure Vessel Code, Section III, Rules for Construction of Nuclear Power Plant Components, Div.5, High Temperature Reactors, ASME (2013)
[8] H.Y. LEE, et al., “High temperature design of finned-tube sodium-to-air heat exchanger in a sodium test loop”, Nuclear Engineering and Design 265 (2013) 833-840.